Generating and absorbing boundary conditions for combined wave-current simulations

Chang, Xing; Akkerman, Ido; Huijsmans, Rene; Veldman, A.E.P.

Publication date
2016

Document Version
Final published version

Published in
Proceedings of the12th International Conference on Hydrodynamics-ICHD 2016

GENERATING AND ABSORBING BOUNDARY CONDITIONS FOR COMBINED WAVE-CURRENT SIMULATIONS

Xing Chang[1]*, Ido Akkerman[1], Rene H.M. Huijsmans[1], Arthur E.P. Veldman[2]

[1]Delft University of Technology, Ship Hydrodynamics and Structures,
Delft, The Netherlands
x.chang@tudelft.nl
I.Akkerman@tudelft.nl
R.H.M.Huijsmans@tudelft.nl

[2]University of Groningen, Mathematics and Computer Science,
Groningen, The Netherlands
a.e.p.veldman@rug.nl

* Corresponding Author

ABSTRACT

The CFD solver ComFLOW is extended to investigate the performance of the Generating and Absorbing Boundary Condition (GABC) in the presence of steady uniform currents. A GABC with currents is introduced that allows the simulation of combined wave-current flow in a truncated domain. This GABC is characterized by a rational approximation of the dispersion relation.

The boundaries where the GABC with currents is applied are transparent to both incoming and outgoing waves superimposed on currents. The absorption properties of the GABC for various waves and currents without objects are analysed in two dimensional domain. The temporal and spatial differences of free surface elevation between the small domain and large domain turn out to be small, i.e. the GABC prevents the reflection from the boundaries well. The large domain here is chosen so that the reflected waves and currents will not reach the outflow boundary of the small domain during the simulation.

1. INTRODUCTION

The combined wave and current condition applies to the study of forces on offshore structures. Therefore, a reliable approach should be chosen in design practice, which takes account of both waves and currents as accurate as possible. In addition, the interaction typically between surface wave-current flow and numerous kinds of man-made offshore structures are local but embedded in a vast domain. For improved computational efficiency, the boundaries are introduced to truncate the large domain so as to obtain a small domain around the structure of interest. Specific boundary conditions should be imposed on these artificial boundaries in such a way that they are open to incoming and outgoing waves (and currents) at the same time.

This topic is explored by developing numerical models based on the Navier-Stokes equations in some literature. The basic idea is to utilize the linear irrotational wave model at the inflow boundary of the domain and to capture the effect of currents on waves as part of the CFD simulation which includes viscous and nonlinear effects. Nevertheless, none of these studies focus on the efficiency of artificial boundary conditions to generate and absorb combined wave-current flow simultaneously, which is addressed in our work. For example, Park et al. (2001) and Markus (2012; 2013) employed a numerical damping zone where the mesh stretching was used, while Teles et al. (2013) imposed a linear increasing viscosity distribution in the extended areas to dissipate the energy of waves.

Similarly, a sponge layer damping method was applied for the vertical velocity component at both domain ends in Zhang et al. (2014). In addition, a breaking-type wave absorber was placed at the tank extremity in Li et al. (2007).

Literature concerning research on open / non-reflective / absorbing boundary conditions is substantially broad extended from different fields over the last few decades. For reviews of ABCs, refer to Tsynkov (1998) and Givoli (2004).

The goal of this research is to allow the simulation of a combined wave-current flow in the truncated domain by extending the CFD solver ComFLOW, which already has an Absorbing Boundary Condition for wave propagation. The mathematical model that describes the fluid flow is present in Section 2. Section 3 shows the formulation of our GABC with current in 2D domain, which also includes the definition of incoming wave-current signal. Simulation results of this GABC for the wave-current flow inside the domain along with related conclusions are included in Section 4. Finally, a few statements for future research have been given in Section 5.

2. MATHEMATICAL MODEL

In our method, the Navier-Stokes equations are solved on a staggered Cartesian grid, where the grid lines are kept aligned with the coordinate axes. The free surface is tracked by the Volume of Fluid (VoF) approach in combination with a local height function. To obtain a solution to the system of partial differential equations, the boundary conditions need to be imposed. At solid boundaries such as structures or bottoms, the Dirichlet condition is applied. The conditions applied at the inflow and outflow boundaries are already developed in ComFLOW to allow waves move into and out of the computational domain simultaneously, called Generating and Absorbing Boundary Conditions (GABC), referred to Wellens (2012) and Duz (2015). Several requirements have been laid out in the aforementioned two studies.

In numerical simulation of relevant practical situations, around five percent reflection for wave components within the frequency band where most of the wave energy resides in the spectrum, is generally an acceptable level of accuracy, since this amount is also encountered in experimental basins and flumes. Hence the 1st-order ABC will be the starting point in our derivation. Another feature in offshore applications is the two-way transparency to waves and currents. This is especially required when a structure is in the domain. Additionally, the extension to three dimensions is not only ‘important’, but also necessary for applications in ComFLOW. Apart from the feasibility of a 3D implementation of the ABC, the computational resources should be marginally compared to the computational effort to determine the solution itself.

The GABC developed in ComFLOW is effectively a Sommerfeld condition, which is perfectly absorbing for one wave component. It was found that the range of absorbed wave components can be extended by replacing the wave speed with a rational approximation of the linear dispersion relation in terms of the wave number. In the derivation of the GABC, linear potential theory has been used extensively to arrive at the final formulation. This GABC without currents forms the basis of our work and more discussion of GABC including currents will be given in the next section.

3. GABC WITH CURRENTS

Since we are looking at the waves and the waves are well described by the potential theory, our boundary condition here is derived from the argument of the potential theory. Considering a constant

current U propagating in the $x-$ direction within a fixed coordinate frame, independent of position and time, we first split off the velocity component from the potential ϕ, i.e. $\phi = \phi_w + Ux$, where ϕ_w is the velocity potential due to linear irrotational waves and Ux is the potential by currents. The currents are arranged in the whole domain initially and waves will be sent into the domain gradually by means of ramping function.

3.1 Wave equation with currents

We know the linear irrotational wave solution ϕ_w

$$\phi_w = [A\cos(kx-\omega t) + B\sin(kx-\omega t)]\frac{\cosh k(z+h)}{\cosh kh} \tag{1}$$

It is found at the free surface

$$g\frac{\partial \phi_w}{\partial z} = -c_0^2\frac{\partial^2 \phi_w}{\partial x^2} \tag{2}$$

holds, where $c_0 = \sqrt{gh\tanh(kh)/kh}$ is the wave speed in the absence of currents.

The linearized kinematic and dynamic conditions at the free surface are as follows

$$\left(\frac{\partial}{\partial t} + U\frac{\partial}{\partial x}\right)\eta_w - \frac{\partial \phi_w}{\partial z} = 0 \tag{3}$$

$$g\eta_w + \left(\frac{\partial}{\partial t} + U\frac{\partial}{\partial x}\right)\phi_w = 0 \tag{4}$$

in which η_w describes the free surface displacement.

Eliminating η_w in Eq. (3) using (4) and using Eq. (2), the wave equation with currents is obtained

$$\frac{\partial^2 \phi_w}{\partial t^2} + 2U\frac{\partial^2 \phi_w}{\partial t \partial x} + (U^2 - c_0^2)\frac{\partial^2 \phi_w}{\partial x^2} = 0 \tag{5}$$

The Eq. (5) can be further factorized as

$$\left(\frac{\partial}{\partial t} + c_-\frac{\partial}{\partial x}\right)\left(\frac{\partial}{\partial t} + c_+\frac{\partial}{\partial x}\right)\phi_w = 0 \tag{6}$$

in which

$$c_- \equiv U - c_0 \quad \text{and} \quad c_+ \equiv U + c_0 \tag{7}$$

In the sequel we will assume that the current is subcritical, i.e. $-c_0 < U < c_0$.

3.2 Conditions at Right and Left Boundary

By means of the method of characteristics, introducing the abbreviation for Eq. (6)

$$\psi_- \equiv \left(\frac{\partial}{\partial t} + c_+\frac{\partial}{\partial x}\right)\phi_w \tag{8}$$

Then Eq. (6) can be rewritten as

$$\left(\frac{\partial}{\partial t} + c_-\frac{\partial}{\partial x}\right)\psi_- = 0 \tag{9}$$

We recognize that ψ_- is constant along the left-running characteristic with the slope $dx/dt = c_- \equiv U - c_0$. At the right-hand boundary, this characteristic is entering the domain. It corresponds with the reflection from that boundary which we do not want. Therefore, ψ_- needs to be specified as

$$\psi_- \equiv \left(\frac{\partial}{\partial t} + c_+\frac{\partial}{\partial x}\right)\phi_w = R^{in} \tag{10}$$

where R^{in} is the characteristic from the incoming waves.

If no incoming waves exist, it would become

$$\psi_- \equiv \left(\frac{\partial}{\partial t} + c_+ \frac{\partial}{\partial x} \right) \phi_w = 0 \tag{11}$$

For the left-hand boundary, we get the following condition in a similar fashion:

$$\psi_+ \equiv \left(\frac{\partial}{\partial t} + c_- \frac{\partial}{\partial x} \right) \phi_w = R^{in} \tag{12}$$

Here ψ_+ is constant along the right-running characteristic with the slope $dx/dt = c_+ \equiv U + c_0$.

Further, ComFLOW solves the Navier-Stokes equations in terms of primitive variables, namely velocity and pressure. Therefore, this condition needs to be expressed in terms of the same variables. Employing the definition of the potential and Bernoulli equation, the following relations could be achieved

$$\frac{\partial \phi_w}{\partial t} = -gz - \frac{p_b}{\rho} - Uu \tag{13}$$

$$\frac{\partial \phi_w}{\partial x} = u = u_b - U \tag{14}$$

Here p_b describes the pressure at the domain boundary and u_b denotes the whole velocity in $x-$ direction at the boundary while u only indicates waves.

Substitution of the relations (13) and (14) into the condition (11) or (12) gives

$$-gz - \frac{p_b}{\rho} - Uu + (U \pm c_0)(u_b - U) = R^{in} \tag{15}$$

3.3 GABC with Currents

The phase speed $c_0 = \sqrt{gh}\sqrt{\tanh(kh)/kh}$ in the condition (15) is only designed for one wave component, but a wave is often composed by superposition of a number of components. Each individual component has its own frequency, amplitude, wave number and phase. Thus, c_0 needs to be approximated for different wave components. The better the dispersion relation is approximated, the less reflection is obtained.

As we know, the wave number k can be found by taking derivatives of the solution in space. By taking the second-order derivation of ϕ_w as in Eq. (1) in $z-$direction, we obtain

$$\frac{\partial^2 \phi_w}{\partial z^2} = k^2 \phi_w \tag{16}$$

Now we introduce a rational polynomial in kh to approximate the dispersion relation as

$$c_0 \approx \sqrt{gh}\, \frac{a_0 + a_1 (kh)^2}{1 + b_1 (kh)^2} \tag{17}$$

Here the coefficients a_0, a_1 and b_1 can be chosen such that different $kh-$ ranges of the dispersion relation are approximated well.

Substituting the relations (16) and (17) into the condition (11) or (12) gives

$$\left[\frac{\partial}{\partial t} + \left(U \pm \sqrt{gh}\, \frac{a_0 + a_1 h^2\, \partial^2 / \partial z^2}{1 + b_1 h^2\, \partial^2 / \partial z^2} \right) \frac{\partial}{\partial x} \right] \phi_w = 0 \tag{18}$$

Further substitution of the expressions (13) and (14) into the above equation leads to the GABC with currents:

$$(1+b_1h^2\,\partial^2/\partial z^2)\left(-gz-\frac{p_b}{\rho}-Uu\right) \\ +[(1+b_1h^2\,\partial^2/\partial z^2)U\pm\sqrt{gh}\,(a_0+a_1h^2\,\partial^2/\partial z^2)](u_b-U)=0 \tag{19}$$

The structure of the discrete form for Eq. (19) bears great resemblance to the pressure Poisson equation inside the domain and can therefore easily be combined.

4. TEST RESULTS

In this section, the above GABC with currents is applied to the problem in the 2D computational domain, where linear regular waves and uniform currents are traveling along the x-direction. The GABC is verified in the wave-only domain by means of the pointwise errors between the results from the truncated domain and the reference solution, followed by the test of GABC with currents. Within the both aforementioned verifications, the comparison between GABC and Sommerfeld condition is carried out as well.

Here we impose the ABC on the right-hand outflow boundary. The wave has a wave length of $\lambda=5m$ and a wave height of $H=0.1m$. With this wave we choose three different water depths: 5, 1 and $0.2\,m$. The coefficients in GABCs are fixed so that the reflection is minimum for the range of kh values between 0 and 6, rather than tuned for a particular kh value. Therefore, the dispersive property of the boundary conditions can be assessed by this test. Different current speeds will be studied, which are 25% and 50% of the wave phase velocity respectively.

The domain lengths for different boundary conditions are given in Table 1. The subscript abc or $somm$ indicates the solution in the small domain using GABC or Sommerfeld condition and the subscript ref denotes the reference solution. In the numerical simulations considered here, the reference result is obtained by solving the problem in a much larger domain with the same discretization in space and time. The length of this larger domain is chosen such that the reflected waves will not pollute the solution in the domain during the simulation.

Table 1: domain length and simulation time

domain	$L_{abc}\,(m)$	4λ
	$L_{somm}\,(m)$	4λ
	$L_{ref}\,(m)$	16λ

The results of the numerical simulations will be analyzed through the pointwise error norm at a single point in Ω, which will be employed to show the difference between the free surface elevations of two calculations, i.e.,

$$e_p=[\eta_{abc}-\eta_{ref}]/H$$

and

$$e_p=[\eta_{somm}-\eta_{ref}]/H$$

4.1 Verification of GABC in wave-only field

The left part in Figure 1 demonstrates the spatial pointwise error e_p at time $t=6T$ caused by ABC and Sommerfeld condition respectively, applied at the outflow boundary in the wave-only domain. e_p is normalized by the wave height $H=0.1m$. Results indicate that the amounts of reflection for both

two conditions are much less than 2% in the whole domain. Moreover, due to the start-up effect where the inflow wave is sent into the domain by ramping function, Sommerfeld condition gives more reflection than ABC since the former is only absorbing the single wave while the latter is tuned to be valid for the wave components in the range of $kh \in (0,6)$.

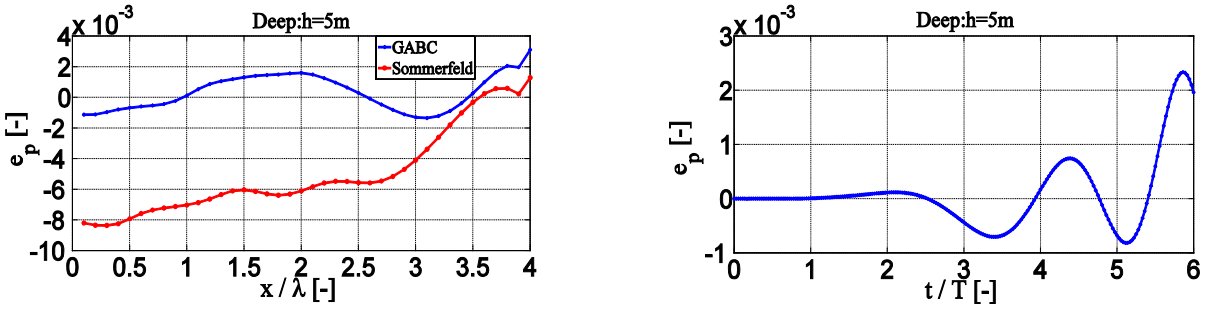

Figure 1: Spatial (left) and temporal (right) pointwise error in wave-only field

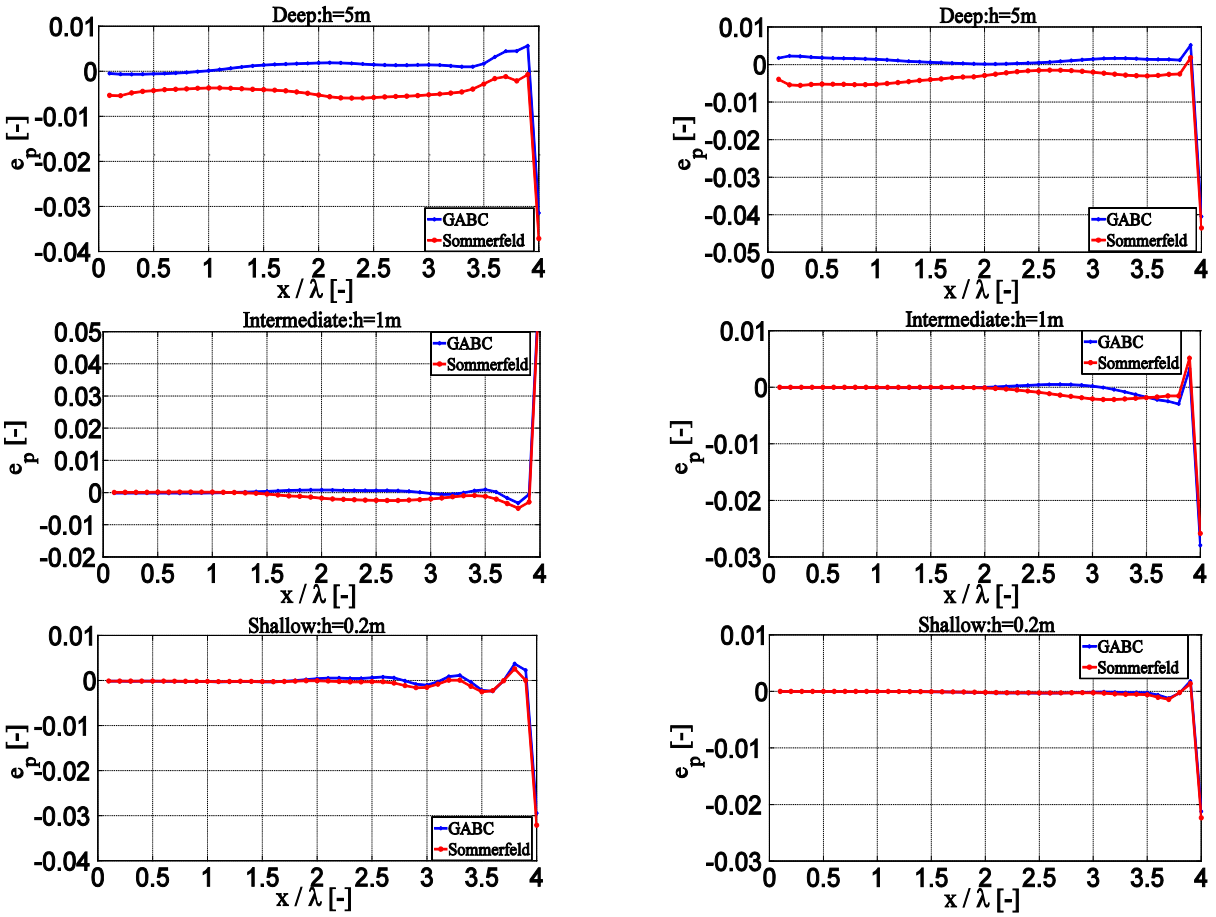

Figure 2: Spatial pointwise error for the case U=0.25c_0(left) and U=0.5c_0(right)

Temporal e_p at position $x = 4\lambda$ (the outflow boundary) caused by ABC is shown in the right part of the Figure 1. The amplitudes of the errors grow in time but remain small after sufficient simulation time. These results are indeed the consequence of the fact that our GABC is preventing the reflection from perturbing the solution in the entire domain.

4.2 Test of GABC in wave-current field

Here the GABC with currents will be tested in the wave-current field for different water depths and current speeds. Figure 2 gives the spatial error distribution at time $t = 8T$ where the left three (from top to bottom) are for the case $U = 0.25c_0$ while the right three for $U = 0.5c_0$. By $t = 8T$, waves and currents have been reflected at the outflow boundary and traveled back to the interior domain. Thus, errors can be observed along the domain. The results for different water depths ($h = 5, 1, 0.2\,m$) are shown from top to bottom, which describe deep, intermediate and shallow water respectively. Again, GABC performs better than Sommerfeld in the top two water depths. As shown in the figure at the bottom, GABC and Sommerfeld give similar reflection since waves become non-dispersive in the shallow water.

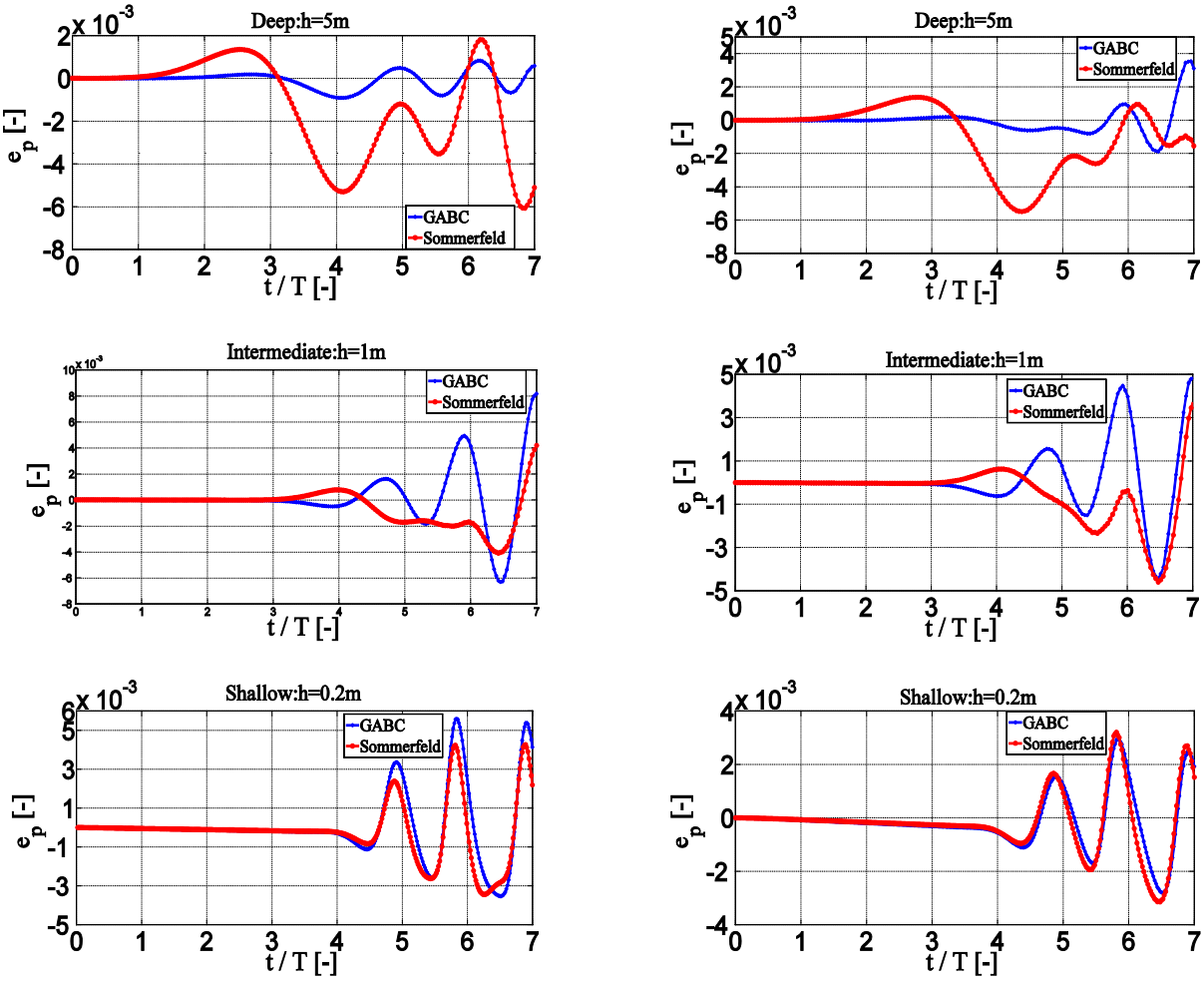

Figure 3: Temporal pointwise error for the case U=0.25c_0 (left) and U=0.5c_0 (right)

The temporal error distributions for different kh values at the outflow boundary $x = 4\lambda$ are illustrated in figure 3. Actually, water will flow out of the domain even before waves reach the boundary since the currents are initially arranged inside the whole domain and reflected at the beginning of simulation. The error resulting from the currents in the beginning is quite small and observed around t = T, 3T and 2T from top to bottom, respectively. The blue lines demonstrate the errors normalized by the wave height in the simulation where GABC is applied, while the red ones give the e_p in the case where the Sommerfeld condition is used. We can observe that the error signal for GABC is more regular than that for the Sommerfeld condition in the top two water depths. However, the errors for both two conditions tend to be close to each other in the shallow water.

5. CONCLUSIONS

This work presents the formulation and preliminary performance of our Generating and Absorbing Boundary Conditions with current. The reflection characteristic in 2D computational domain is observed. The extension of GABC into a 3D domain will be the next step. After the tests with linear waves, the verification of our model for nonlinear waves and currents is going to be taken. At last, the combined wave-current loads on structures will be investigated.

REFERENCES

Zhang, J.S., Zhang, Y., Jeng, D.S., Liu, P.L.F. and Zhang, C., 2014. Numerical simulation of wave-current interaction using a RANS solver, Ocean Engineering 75, p. 157-164.
Wellens, P., 2012. *Wave simulation in truncated domains for offshore applications*, Delft, p. 75-97.
Umeyama, M., 2005. Reynolds stresses and velocity distributions in a wave-current coexisting environment, Waterway Port and Coastal Ocean Engineering 131, p. 203-212.
Umeyama, M., 2009. Changes in turbulent flow structure under combined wave-current motions, Waterway Port and Coastal Ocean Engineering 135, 213-227.
Umeyama, M., 2011. Coupled PIV and PTV measurements of particle velocities and trajectories for surface waves following a steady current, Waterway Port and Coastal Ocean Engineering 137, p. 85-94.
Tsynkov, S., 1998. Numerical solution of problems on unbounded domains: a review, Applied Numerical Mathematics 27, p. 465-532.
Toffoli, A., Waseda, T., Houtani, H., Kinoshita, T., Collins, K., Proment, D., Onorato, M., 2013. Excitation of rogue waves in a variable medium: an experimental study on the interaction of water waves and currents, Physical Review E 87, 051201.
Teles, M.J., Pires-Silva, A.A., Benoit, M., 2013. Numerical modelling of wave-current interactions at a local scale, Ocean Engineering 68, p. 72-87.
Park, J.C., Kim, M.H., Miyata, H., 2001. Three-dimensional numerical wave tank simulations on fully nonlinear wave-current-body interactions, Marine Science and Technology 6, p. 70-82.
Markus, D., Hojjat, M., Wuchner, R. and Bletzinger, K.U., 2012. A numerical wave channel for the design of offshore structures with consideration of wave-current interaction, Proceedings, 22th International Offshore and Polar Engineering Conference, p. 695-702.
Markus, D., Wuchner, R. and Bletzinger, K.U., 2013. A numerical investigation of combined wave-current loads on tidal stream generators, Ocean Engineering 72, p. 416-428.
Li, T., Troch, P., Rouck, J.D., 2007. Interactions of breaking waves with a current over cut cells, Journal of Computational Physics 223, p. 865-897.
Givoli, D., 2004. High-order local non-reflecting boundary conditions : a review, Wave Motion 39, p. 319-326.
Duz, B., 2015. *Wave generation, propagation and absorption in CFD simulation of free surface flows*, PhD thesis, Delft, p. 29-72.

ACKNOWLEDGEMENT

The research is supported by the Dutch Technology Foundation STW, applied science division of NOW and China Scholarship Council (CSC).